Cosmc is an essential chaperone for correct protein O-glycosylation

Yingchun Wang[a], Tongzhong Ju[a,1], Xiaokun Ding[a], Baoyun Xia[b], Wenyi Wang[a], Lijun Xia[c], Miao He[b], and Richard D. Cummings[a,1]

Departments of [a]Biochemistry and [b]Human Genetics, Emory University School of Medicine, Atlanta, GA 30322; and [c]Cardiovascular Biology Research Program, Oklahoma Medical Research Foundation, Oklahoma City, OK 73104

Cosmc is a molecular chaperone thought to be required for expression of active T-synthase, the only enzyme that galactosylates the Tn antigen (GalNAcα1-Ser/Thr-R) to form core 1 Galβ1–3GalNAcα1-Ser/Thr (T antigen) during mucin type O-glycan biosynthesis. Here we show that ablation of the X-linked Cosmc gene in mice causes embryonic lethality and Tn antigen expression. Loss of Cosmc is associated with loss of T-synthase but not other enzymes required for glycoprotein biosynthesis, demonstrating that Cosmc is specific in vivo for the T-synthase. We generated genetically mosaic mice with a targeted Cosmc deletion and survivors exhibited abnormalities correlated with Tn antigen expression that are related to several human diseases.

galactosyltransferase | Tn antigen | null mutation | genetic mosaicism | X chromosome

Mucin-type O-glycans are synthesized in the Golgi apparatus by sequential glycosyltransferase reactions all deriving from a common precursor GalNAcα1-Ser/Thr-R (Tn antigen). Core 1 O-glycan Galβ1–3GalNAcα1-Ser/Thr (T antigen) is the most common O-glycan core (1), and is synthesized by a single mammalian enzyme termed the core 1 β3galactosyltransferase (core 1 β3GalT or T-synthase), which transfers galactose from the donor UDP-Gal to Tn antigen (2). The T-synthase is an unusual enzyme, as its active expression appears to depend on coexpression with an unusual molecular chaperone termed "Cosmc" (core 1 β3GalT specific molecular chaperone) (3). We showed that Cosmc is an endoplasmic reticulum (ER)-localized molecular chaperone that prevents aggregation and proteasomal degradation of nascent T-synthase (4) and can directly interact with denatured T-synthase (5). Individuals with Tn syndrome exhibit acquired mutations in Cosmc in blood cell precursors, and appear normal in nonhemapoietic tissues (6, 7). However, it is not known whether defects in germ-line Cosmc expression would be associated with observable phenotypes, and whether Cosmc acts as a chaperone to other glycosyltransferases or proteins within the secretory pathway.

To this end, we generated mice with disrupted Cosmc, an X-linked gene at Xc3, ranging from complete to partial disruption in mosaic animals. Mice lacking Cosmc expressed the Tn antigen and exhibited a variety of phenotypes ranging from embryonic death, gross growth retardation, and apparent normal development, depending on the extent of Cosmc deletion. These engineered animals provide a unique model for exploring the biological consequences of Tn antigen expression in human diseases.

Results

Generation of Cosmc-Null and Cosmc-Floxed Mouse ES Cells.
We engineered a targeting vector with three Lox[P] sites in the murine Cosmc allele, which flanked the exon (ORF) and an inserted Neo cassette (Fig. 1A). After transfection and selection of ES cells (HZ2.2, derived from a male 129SvEv/TAC mouse embryo) and screening with PCR, eight clones with the correct homologous recombination were obtained and confirmed by Southern blot (Fig. S1). To generate Cosmc-null (Cosmc$^{-/y}$) and floxed Cosmc (Cosmc$^{flox/y}$) ES cells, one of eight clones was transiently transfected with a plasmid expressing Cre recombinase. After selection, four clones with deletion of both

Cosmc ORF and the Neo-gene (Cosmc$^{-/y}$), and another clone with deletion of Neo-gene only (Cosmc$^{flox/y}$) were obtained, and confirmed by Southern blot (Fig. 1B). WT ES cells have T-synthase activity, but Cosmc-null ES cells lack T-synthase activity (Fig. 1C). Moreover, Cosmc-null ES cells express Tn antigen on their surfaces, as detected by anti-Tn mAb in immunohistochemistry (IHC) (Fig. 1D). RT-PCR confirmed that Cosmc-null ES cells lack Cosmc transcripts (Fig. 1E). These results show that targeted deletion of Cosmc causes loss of T-synthase activity and Tn antigen expression.

Loss of Cosmc Does Not Affect Other Types of Protein Glycosylation.
To determine if Cosmc deletion affects other glycosylation pathways, we assessed protein glycosylation in two ways. We explored protein glycosylation using plant lectins of known specificities, and which recognize many different types of glycans; in a second approach we performed mass spectrometry profiling of N-glycans in WT and Cosmc-null ES cells. First, we analyzed total glycoproteins before and after treatment with either sialidase (S), sialidase plus O-glycanase (O), which is specific for releasing the nonsialylated T antigen, or N-glycanase (P), which can release all types of N-glycans. Helix pomatia agglutinin (HPA) (8) binds to the Tn antigen control and many glycoproteins in the Cosmc$^{-/y}$ ES cells, but did not bind glycoproteins from WT cells (Fig. S2A), showing that loss of Cosmc results in expression of the Tn antigen on many different glycoproteins. Interestingly, peanut agglutinin (PNA) from Arachis hypogaea, which binds the T antigen (9), did not bind glycoproteins from either WT ES or Cosmc-knockout (KO) ES cell extracts (Fig. S2B). As controls, we included human Jurkat cells, which have a mutation in Cosmc and express Tn antigen (3, 10), and Jurkat cells transfected with WT Cosmc and which express glycoproteins that bind PNA after sialidase treatment (Fig. S2B). Thus, the O-glycans on WT ES cells are likely to be complex O-glycans, such as core 2-related or extended core 1 structures. We also analyzed binding of other plant lectins that recognize a wide variety of glycan structures, including Canavalia ensiformis agglutinin (Fig. S2C), a lectin that binds mannose on N-glycans (11); Ricinus communis agglutinin-1 (Fig. S2D), a lectin that binds galactose on N- and O-glycans (12, 13); and Sambucus nigra agglutinin (Fig. S2E), a lectin that binds α2–6 sialic acid (14). The binding of all three lectins was generally similar toward glycoproteins from Cosmc$^{-/y}$ cells compared with the Cosmc$^{+/y}$ cells and after glycosidase treatments. These results demonstrate that terminal glycosylation in the Golgi apparatus by a variety of glycosyltransferases, especially those in N-glycosylation pathways, are not demonstrably affected by deletion of Cosmc.
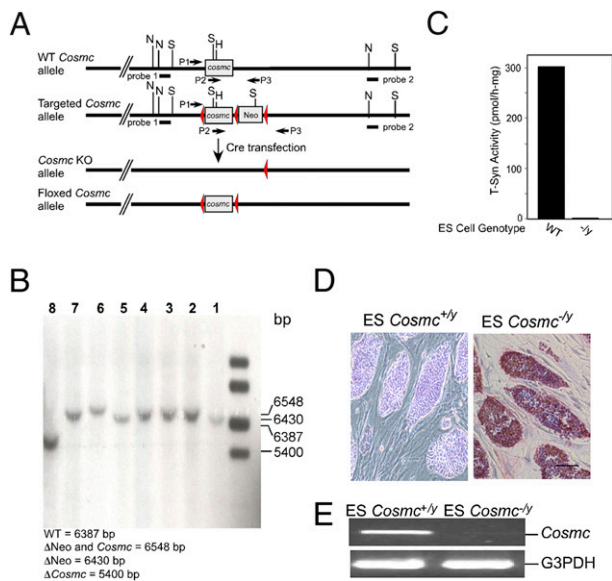
Fig. 1. Creation and characterization of ES cells with a null *Cosmc* and floxed *Cosmc*. (*A*) Schematic of targeted deletion strategy. (*B*) Southern blot confirmation of the genotypes of the constructs. (lanes 1 and 5) WT ES cells; (lanes 2, 3, 4, and 6) ES clones with deletion (Δ) of both *Neo* and *Cosmc* genes; (lane 7) ES clone with deletion of Neo gene only; (lane 8) ES clone with deletion of Cosmc only. (*C*) T-synthase activity assay of WT and Cosmc KO ES cells. Data show average of two replicates within one experiment. (*D*) IHC of ES cells with anti-Tn mAb (red represents Tn antigen expression). (Scale bar, 50 μm.) (*E*) RT-PCR of transcripts from WT and KO cells.

We also performed structural analysis of N-glycans released from the total membrane proteins of both WT and *Cosmc$^{-/y}$* ES cells using MALDI-TOF mass spectrometry. This process revealed that the N-glycans from WT ES cells have compositions that indicate they are mainly high mannose-type, ranging from Man$_5$GlcNAc$_2$ to Man$_9$GlcNAc$_2$ (Fig. S3*A*), with minor complex-type structures, in which the sialylated fraction is shown (*Inset* of Fig. S3*A*). Importantly, the N-glycan profile from *Cosmc*-KO ES cells is similar to that from WT ES cells, demonstrating that N-glycans remain unchanged after *Cosmc* depletion (Fig. S3*B*). These results are consistent with the N-glycome of mouse ES cells published by Amano et al. (15), who showed that high mannose-type N-glycans, Man$_5$GlcNAc$_2$ to Man$_9$GlcNAc$_2$, account for 78% of the total, with complex-type glycans as a minority. The combined results of lectin blotting and mass spectrometry demonstrate that deletion of *Cosmc* in ES cells affects O-glycan biosynthesis, and not N-glycan structures.

Lack of Viable *Cosmc*-Null Mice (*Cosmc$^{-/y}$*). To study the function of *Cosmc* in mouse development, we attempted to generate *Cosmc*-null mice. *Cosmc*-null ES cells *(Cosmc$^{-/y}$)* were microinjected into C57BL/6J blastocysts, which were then implanted into pseudopregnant mice. Two chimeric pups with a high percentage of agouti (*Cosmc$^{-/y, +/y}$*) were produced, but they died shortly after birth. Three additional chimeras with medium and low percentage agouti were produced, but they did not exhibit germ-line transmission of *Cosmc$^{-/y}$*. We repeated three microinjections using a lower percentage of *Cosmc*-null ES cells from all three clones with a null *Cosmc*, and a total of eight chimeras (two to three chimeras per clone) were generated; however, only low-to-medium percentage agouti were obtained. The chimeras were then bred with C57BL/6J female mice. From a total of 136 mice from 18 litters, none of them expressed an agouti coat color. These results indicate that chimeras with *Cosmc$^{-/y, +/y}$* are not germ-line-transmissible. As a control for these experiments, chimeras with floxed *Cosmc* were generated from the same procedure and were germ-line-transmissible. Thus,

these observations strongly suggest that disruption of *Cosmc* in mice causes embryonic lethality.

To study the function of *Cosmc* in development and in specific tissues, male ES cells carrying the floxed *Cosmc* allele (*Cosmc$^{flox/y}$*), were microinjected into C57BL/6J blastocysts and subsequently implanted into pseudopregnant mice. Chimeras among the offspring were bred with C57BL/6J mice. Female mice with a single floxed *Cosmc* (*Cosmc$^{flox/+}$*) and male mice with a floxed *Cosmc* (*Cosmc$^{flox/y}$*) were generated, which were then bred with each other to create females with fully-floxed *Cosmc* (*Cosmc$^{flox/flox}$*).

To assess the expression of *Cosmc* and whether the Lox^P sites affect the transcription and mRNA processing or splicing, we performed semiquantitative RT-PCR covering 5′-end noncoding exon and a portion of the ORF, using the mRNA isolated from kidney and spleen in WT mice and transgenic animals (*Cosmc$^{flox/+}$* or *Cosmc$^{flox/flox}$*). The results show that transcription of Lox^P-*Cosmc* was unchanged in terms of the size and level in kidney and spleen between WT and transgenic animals (Fig. S4*A*) and sequences of RT-PCR products were confirmed.

Mosaic Mice with a Null *Cosmc* Exhibited a Variety of Gross Phenotypes, and a Diversity of Expression of Tn Antigen in Many Tissues. To create mice having a null *Cosmc* mutation, either in all cells or in subsets of cells, we chose a strategy whereby *Cosmc* is deleted in *EIIa-Cre* transgenic mice, as used for generating mosaic animals for the essential X-linked *PIGA* gene (16). In this model, deletion of *Cosmc* is mediated by *Cre* expression under control of the adenovirus *EIIa* promoter; thus, expression requires the natural transcriptional factor E1a, whose expression is restricted to oocytes and preimplantation embryos (17). This stochastic process results in loss of *Cosmc* in some but not all cells. We generated breeding pairs of *Cosmc$^{+/flox}$* female and *EIIa-Cre* male (four breeding pairs) (Fig. 2*A*) that resulted in the generation of 12 litters with 127 pups and a litter size between 6 and 12, which is within the normal range. Through this breeding strategy, the genotype of the offspring will be either WT or mosaic.

From these mosaic offspring (male: *Cosmc$^{-/y, (flox/y)}$*, female: *Cosmc$^{+/-(flox/+)}$*) we observed a surprising range of phenotypes, which could be generally assigned to two groups. The Group I Mosaics (Table 1) exhibited an obvious gross phenotype, including smaller body size; hemorrhages in brain, lung, and intestine; bloody chylous ascites; Tn(+) blood cells; and splenomegaly. IHC staining with anti-Tn mAb revealed a significant amount of Tn(+) cells in many tissues, such as spleen, heart, lung, gastrointestinal (GI) tract, liver, and kidney (Fig. 2*B*). In kidney, the Tn(+) cells were found in glomeruli in the cortex and proximal and distant tubules. The Group I mosaics suffered ~30% mortality within 2 weeks. By contrast, Group II Mosaics (Table 1) appeared "normal" and had a low degree of Tn antigen expression in several tissues, such as blood (<5%) and several organs. The variable and complicated phenotype from the mosaic animals could be predicted to arise from: (*i*) low or medium mosaicism, because of the incomplete deletion of the Cosmc gene in both male and female mosaics, as the *Cre* expression was narrowed in embryonic day (E) 2.5 to E4.5; or (*ii*) the variable nature of X-chromosome inactivation in females, because only floxed alleles from the mother (the other WT allele is from the father, *EIIa-Cre* mouse) could be deleted by the *Cre*-mediated DNA homologous recombination.

Southern blot analyses (Fig. S4 *B–D*) were performed to define the degree of deletion of *Cosmc* from multiple organs. In Group II Mosaics, there was a less intense band of *Cosmc* (deleted) in several organs (Fig. S4*C*) because of the partial deletion, whereas in Group I Mosaics almost half of the *Cosmc* DNA appeared as a deleted genotype (Fig. S4*B*), representing about half of the cells from those organs. Furthermore, anti-Tn IHC staining showed that a major portion of most of the organs was Tn(+) from Group I Mosaic mice (Fig. 2*B*), whereas a minor portion of the cells was Tn (+) from Group II mosaic animals (Fig. 2*C*). There was no sig-
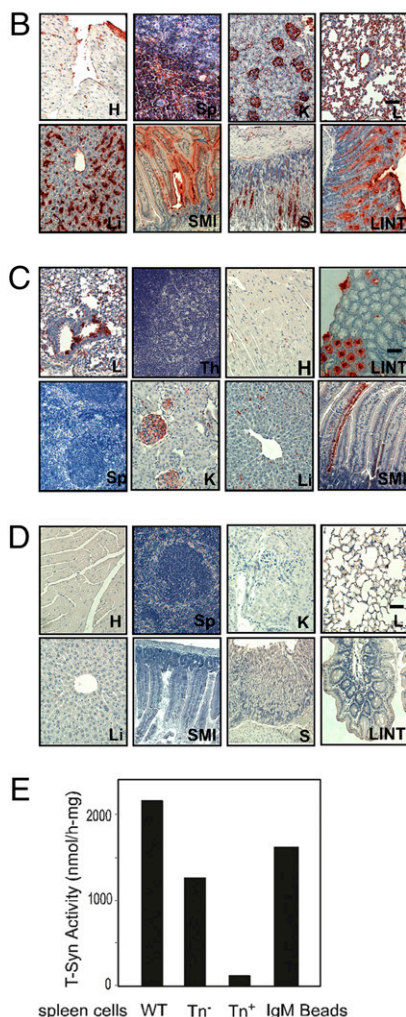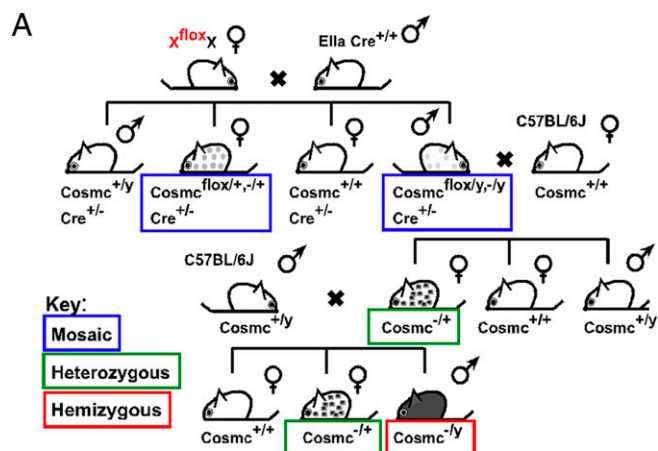
Fig. 2. Creation and characterization of mosaic mice, Tn(+) cells in multiple tissues from mosaic mice. (*A*) Schematic of breeding strategies for generating *Cosmc* mosaic, heterozygous, and hemizygous KO mice. Mosaic genotypes are boxed in blue, heterozygous genotypes are boxed in green, and hemizygous genotypes are boxed in red. (*B–D*) IHC of the degree of Tn antigen expression from multiple organs, including heart (H), spleen (Sp), kidney (K), liver (Li), lung (L), small intestine (SMI), large intestine (LINT), stomach (S), and thymus (Th) for Group I Mosaics (*B*); Group II Mosaics (*C*); WT littermate controls (*D*). Brown represents Tn antigen expression in IHC. (Scale bar = 50 μm.) (*E*) T-synthase activity in splenocytes from WT animals and both Tn(+) and Tn(−) cells from mosaic animals. Data shows average of two replicates within one experiment.

Table 1. Summary of mosaic mice created by breeding of female mice (*Cosmc*flox/+) with *Ella-Cre* male mice

	Group I (n = 7)	Group II (n = 10)
Growth	Growth retardation	No obvious difference vs. litter mates
Hemorrhage	Brain, lung, intestine, bloody ascites	None
% Tn- peripheral blood	>5%	<5%
Splenomegaly	60%	20% mice age >28 weeks
No. of organs with high Tn expression	>3	N/A
Mortality postnatal 2 weeks	28.5%	None

nificant Tn staining in WT animals from the littermate control (Fig. 2*D*). These data demonstrate that Tn expression is correlated with *Cosmc* deletion.

Tn(+) Cells Isolated from Tissues of Mosaic Mice Lack T-Synthase Activity. To directly define whether Tn expression correlated with loss of T-synthase in the mosaic mice, the splenocytes with both Tn (+) and Tn(−) phenotype were immuno-isolated from the male animals using anti-Tn beads, and the T-synthase activity was measured. Although splenocytes from WT animals and Tn(−) splenocytes from mosaic animals had robust T-synthase activity, Tn(+) splenocytes lack activity (Fig. 2*E*). Taken together, these results show that *Cosmc* regulates O-glycosylation in vivo through T-synthase activity.

Offspring Generated from Mosaic Male Mice and Heterozygous Female Mice Exhibited Unbalanced Sex Ratio and a Variety Of Abnormalities. To get a clearer picture of *Cosmc* function in vivo, mice with a single or pure genotype are desirable. We chose a strategy (Fig. 2*A*) to create heterozygous female mice ($Cosmc^{+/-}$) by segregated breeding of mosaic male mice ($Cosmc^{-/y,flox/y}$) from Group II Mosaic mice with C57BL/6J female mice. In total, 112 pups were obtained, and their genotype and gender are summarized in Table S1. The ratio of females to males was 1.6:1, in contrast to the expected 1:1 ratio ($P < 0.01$), and the χ^2 statistic of Mendelian segregation was $x^2 = 11.8$. The $Cosmc^{+/-}$ females had a similar and variable phenotype as seen for the mosaic mice, including postnatal death, growth retardation, and apparent normal development. Histological staining with anti-Tn mAb revealed the clonal expression of Tn antigen in many tissues, such as kidney, lung, small intestines, and large intestines, with a similar expression pattern seen in mosaic mice (Fig. S4 *E–H*).

Because this strategy could only generate heterozygous female mice, and all of the males were WT, we used another strategy in which the heterozygous female mice ($Cosmc^{+/-}$) were bred with C57BL/6J male ($Cosmc^{+/y}$) mice. This approach was designed to create WT males ($Cosmc^{+/y}$, expected 25%) and females ($Cosmc^{+/+}$, expected 25%), heterozygous females ($Cosmc^{+/-}$, expected 25%), and hemizygous males ($Cosmc^{-/y}$, expected 25%). A total of 105 (91 WT plus 14 heterozygous) pups were born (Table S2). The genotypes were $Cosmc^{+/y}$ male, $Cosmc^{+/+}$ female, and $Cosmc^{+/-}$ female; the ratio of female to male animals was ~2:1; and there were no animals with the genotype $Cosmc^{-/y}$. These results indicate that disruption of the active *Cosmc* allele results in embryonic lethality.

Male Mouse Embryos (Cosmc−/y) Die at E10.5–E12.5 and Express Tn Antigen, Whereas Heterozygous Female Mouse Embryos (*Cosmc*+/−) Exhibit Diverse Phenotypes. To confirm whether the lack of offspring with a null *Cosmc* genotype ($Cosmc^{-/y}$) resulted from em-

bryonic lethality, we examined the embryos from apparent normal $Cosmc^{+/-}$ female mice bred with C57B/6J male mice. The pregnant $Cosmc^{+/-}$ mice were monitored and embryos at E9 to E15 from timed mating were analyzed by dissection microscopy. At E9.5, $Cosmc^{-/y}$ embryos appeared developmentally normal, but thereafter they developed progressive hemorrhaging in the brain and spinal cord from E10.5 to E12.5 (Fig. 3A) and exhibited growth retardation, and many dead embryos were observed. Because embryos with a null $Cosmc$ died early, it was not feasible to assess whether there were defects in organogenesis. Interestingly, we observed variations in $Cosmc^{-/y}$ embryos at E11 and E12 (Fig. 3B). Some $Cosmc^{-/y}$ embryos were dead; others exhibited hemorrhaging in the brain and spinal cord. Nevertheless, by E12.5 all 20 $Cosmc^{-/y}$ embryos died. Interestingly, 7 of 25 heterozygous females ($Cosmc^{+/-}$) were dead at E12.5 because of hemorrhaging, as seen in $Cosmc^{-/y}$ mice. Three of the remaining 6 survived to E14.5 with hemorrhaging and disorganization of the vascular system

Table 2. Summary of the embryos from heterozygous female ($Cosmc^{+/-}$) mice bred with C57BL/6J male ($Cosmc^{+/y}$) mice

|	$Cosmc^{+/+}$ or $Cosmc^{+/y}$	$Cosmc^{+/-}$ (Hemorrhage)	$Cosmc^{-/y}$ (Hemorrhage + embryonic death)
E8.5–E9.5	6	10	8
E10.5–E12.5	43	25 (7*)	20 (20*)
E14.5	10	6 (3*)	0

*Embryos with hemorrhage.

in the body, although they appeared developmentally normally other than hemorrhaging; the remaining heterozygous female mouse embryos looked normal by E14.5 (Table 2). The hemorrhage phenotype of $Cosmc$-null mice is similar to that in the *T-synthase* KO mouse (18, 19), although $Cosmc$-null embryos died 1 to 2 days earlier than that observed for *T-synthase* KO mouse embryos.

T-synthase activity was not detectable in $Cosmc^{-/y}$ embryos (Fig. 3C), although the activity in $Cosmc^{+/-}$ female embryos varied depending on the animal, and WT embryos had high activity. As a control, another galactosyltransferase (β1–4GalT), which like T-synthase is a Golgi enzyme and utilizes UDP-Gal as a donor, remained unchanged in all embryos examined. Importantly, T-synthase protein was missing in the hemizygous embryos ($Cosmc^{-/y}$), probably because of its misfolding and degradation via ER-associated degradation pathway, and T-synthase protein was detected as doublet bands in both WT embryos and heterozygous embryos (Fig. S5). This observation is consistent with what was shown for purified T-synthase from rat liver (20). This lower band of the doublet may result from the cleavage of the full-length T-synthase protein, but further characterization is required. Nevertheless, these results support the conclusion that Cosmc is a specific molecular chaperone for the T-synthase and that targeted deletion of $Cosmc$ in animals is correlated with loss of both T-synthase protein and activity.

To determine whether the loss of $Cosmc$ affected O-glycan structures in vivo, we probed blots of embryonic extracts with PNA (Fig. 3D) for the T antigen and HPA (Fig. 3E) for the Tn antigen. PNA bound to many glycoproteins from $Cosmc^{+/+}$ and $Cosmc^{+/y}$ embryos following sialidase treatment, although there was less intense staining as might be expected with the heterozygote $Cosmc^{+/-}$, but there was no binding to glycoproteins from $Cosmc^{-/y}$ embryos. By contrast, HPA bound to many glycoproteins from $Cosmc^{-/y}$ embryos and showed less intense binding to the heterozygote $Cosmc^{+/-}$; there was no significant binding to glycoproteins from $Cosmc^{+/+}$ and $Cosmc^{+/y}$ embryos. Enzymatic desialylation by sialidase treatment of glycoproteins from embryo extracts was required to expose binding sites for PNA, indicating that sialic acid capped most core 1 structures to form the sialyl T antigen or disialyl T antigen. Desialylation of glycoproteins from $Cosmc^{-/y}$ and $Cosmc^{+/-}$ embryos increased the staining intensity for HPA, suggesting the presence of the sialyl Tn antigen. To confirm the recognition of PNA and HPA for the T antigen and Tn antigens, respectively, we explored the binding of biotinylated PNA and HPA on a glycan microarray from the Consortium for Functional Glycomics. PNA at both 1 and 10 μg/mL showed the highest binding to glycans containing Galβ1–3GalNAc-R (Fig. S6), whereas HPA at both 1 and 10 μg/mL showed highest binding to glycans containing terminal GalNAcα1-R. These lectin concentrations were chosen because they are in the range of those used in IHC and Western blots.

Tn Antigen Is Expressed by All Cells in the Null $Cosmc$ Embryo. We performed whole-mount staining of the whole embryos with Alexa488-labeled anti-Tn antibody. Although the WT animal had no detectable staining, the whole $Cosmc^{-/y}$ embryo was Tn antigen-positive; however, there were discernable differences in the intensity of Tn expression in different regions of the embryo
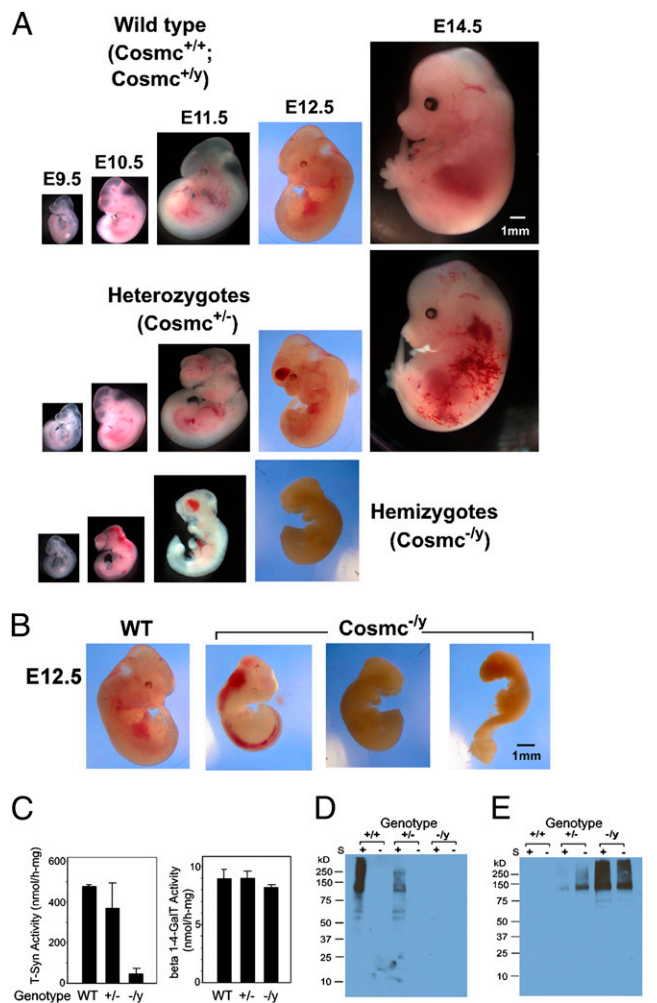
Fig. 3. Disruption of $Cosmc$ in mice results in embryonic lethality and Tn antigen expression. (A) Embryos photographed at E9.5, E10.5, E11.5, E12.5, and E14.5 from WT, heterozygous, and hemizygous genotypes, demonstrating normal growth (WT) vs. hemorrhage and early death (heterozygous and hemizygous, respectively). (Scale bar, 1 mm.) (B) At E12.5, comparison of WT (healthy) vs. hemizygous (hemorrhagic, panel 2 and dead, panels 3 and 4). (Scale bar, 1 mm.) (C) T-synthase activity and β4 GalT activity in WT (2), heterozygous (3), and hemizygous (3) embryos. Data show the average of the number of noted embryos in parentheses ± 1 SD. (D and E) Embryonic extracts probed with PNA (D) and HPA (E) with and without Sialidase (S) treatment. The same amount of protein from the extracts of WT, heterozygous, and hemizygous embryos were analyzed in each lectin blot.

DEVELOPMENTAL BIOLOGY
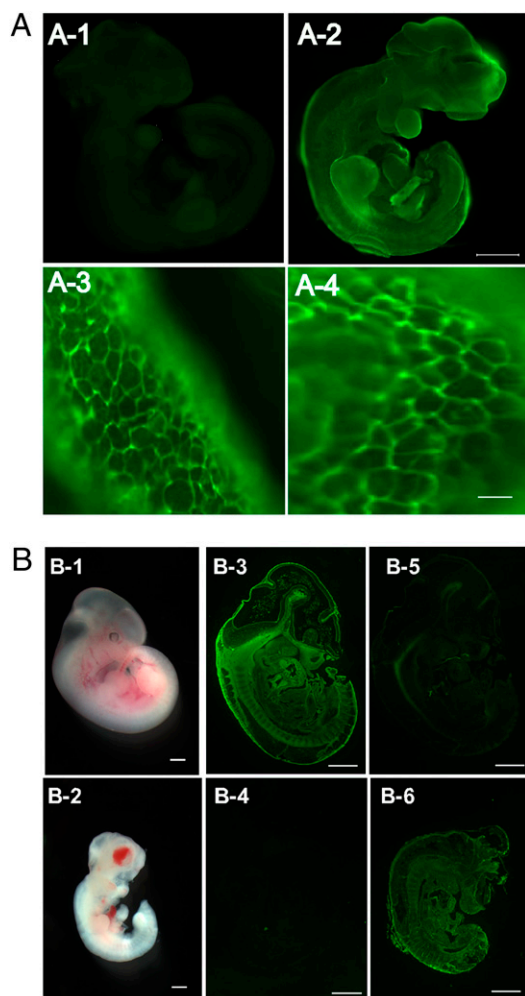
Fig. 4. Whole-mount staining with Tn antibody (*A*) and lectins (*B*) revealed universal Tn antigen expression on the surface of every cell in *Cosmc$^{-/y}$* embryos at E10.5. (*A1*) Whole embryo from WT animal, (*A2*) whole embryo of *Cosmc$^{-/y}$* animal; green represents Tn antigen expression. (Scale bar, 500 μm.) (*A3* and *A4*) Dissections of *Cosmc$^{-/y}$* embryo under fluorescent microscopy at 20× magnification. (Scale bar, 10 μm.) (*B1–B6*) Whole embryos photographed at E11.5 from WT (*B1*) and *Cosmc$^{-/y}$* (*B2*). E11.5 embryo sections from WT (*B3* and *B5*) and *Cosmc$^{-/y}$* (*B4* and *B6*) were stained with biotinylated lectins PNA (*B3* and *B4*) and HPA (*B5* and *B6*), detected with fluorescent streptavidin. (Scale bar, 1 mm.)

(Fig. 4 *A1* and *A2*). All Tn(+) cells from *Cosmc$^{-/y}$* embryos were surface illuminated as rings connected to form a network-like structure (Fig. 4 *A3* and *A4*). These results show that Tn antigen is localized on the cell surface and in the extracellular matrix where most mucin type O-glycosylated glycoproteins likely reside. Embryos from E11.5 (Fig. 4 *B1* and *B2*) were sectioned and stained with PNA and HPA lectins and show PNA binding to the WT embryonic tissue following sialidase treatment (Fig. 4*B3*) and was not bound by HPA (Fig. 4*B5*). In contrast, the *Cosmc$^{-/y}$* embryo sections lost PNA binding (Fig. 4*B4*) but shows high binding to HPA (Fig. 4*B6*). This is a unique example of the presence of a mucin type O-glycan antigen on all identifiable cells in an organism and strongly suggests that mucin type O-glycosylation occurs in most cells during mouse embryonic development, at least up to the E9 to E15 stage.

Discussion

Early studies on the chaperone function of Cosmc in cultured cells showed that Cosmc expression is required for formation of active

T-synthase (3, 4, 10, 21). Thus, a major question in our studies on Cosmc was whether Cosmc is specific for the T-synthase and whether targeted deficiency of *Cosmc* leads to loss of expression or function of other proteins or glycoproteins within the secretory pathway. Because mouse ES cells are male and hemizygous for *Cosmc*, we could use these cells to examine the consequences of complete *Cosmc* loss on protein glycosylation. The complex biosynthesis of glycoproteins requires the activities of many dozens of enzymes in the ER, Golgi, and other organelles in the secretory pathway, including nucleotide sugar transporters, glycosidases, glycosyltransferases, and other chaperones involved in glycoprotein assembly and movement to the cell surface (22–26). We found that although mouse ES cells with a null *Cosmc* lack T-synthase activity and express Tn antigen, all other protein glycosylation, including total N-glycan profiles by mass spectrometry, and cell growth appeared normal in vitro. Thus, the evidence demonstrates that in vivo the major client of Cosmc is the T-synthase and that loss of Cosmc function is associated with loss of T-synthase activity, without obvious changes in other aspects of protein glycosylation.

Mouse embryos with a *Cosmc*-null genotype lacked T-synthase activity and expressed Tn antigen on the surface of every observable cell, whereas WT mice expressed sialyl T antigen as assessed by PNA staining after desialylation. *Cosmc*-null animals died at E10.5 to E12.5, with the most obvious phenotype being hemorrhaging in the brain and spinal cord. The mosaic mice and heterozygous female mice were viable and survivors displayed a variety of gross phenotypes, ranging from postnatal death, growth retardation, and splenomegaly, to apparent normal development, depending on the extent of *Cosmc* deletion, and corresponding expression of the Tn antigen, in many tissues. This study is unique in showing that *Cosmc* is essential for mouse development and that experimental depletion of *Cosmc* causes loss of T-synthase activity and Tn antigen expression in vivo.

The phenotype of mouse embryos with a null *Cosmc* varied depending on the sex and the degree of *Cosmc* loss in heterozygous females. Embryos with null mutations in *Cosmc* die from hemorrhaging in the brain and spinal cord, which resemble the phenotypes of the *T-synthase* KO (18, 19). Interestingly, mouse embryos with a null *Cosmc* die at E10.5 to E12.5, although mice with *T-synthase* KO die at E13.5. This slightly earlier embryonic death of *Cosmc*-null animals could be a result of one of several factors, because the deletion of *Cosmc* is fundamentally different from deleting T-synthase. *T-synthase* mRNA and protein might have a longer half-life than *Cosmc*. Loss of Cosmc could result in misfolded T-synthase, whose accumulation could lead to unfolded protein response and ER-associated degradation, which is associated with enhanced cellular apoptosis (27). Alternatively, lack of Cosmc function and the nonproductive association of ER chaperones with misfolded T-synthase could indirectly lead to altered folding of other ER client molecules. For example, in cell lines lacking Cosmc, we found that the accumulated T-synthase is associated with GRP78 (4). In contrast, T-synthase protein in the hemizygous embryos (*Cosmc$^{-/y}$*) was degraded efficiently and no detectable T-synthase protein accumulated. Interestingly, the hemizygous male (*Cosmc$^{-/y}$*) mouse embryos died from E10.5 to E12.5, rather than all on the same day, although they have the same genotype and are derived from the same litter. This phenomenon could be because of the X-chromosome inactivation status in the oocytes (*Cosmc$^{+/-}$*) before meiosis. For example, male embryos from the oocytes using the null *Cosmc* as an active allele could die earlier than those from oocytes using the WT *Cosmc* as an active allele, in which the mRNA of *Cosmc* from oocytes persists some time before completely degrading in the embryo after fertilization.

Mosaic mice with dominant deletion of *Cosmc* developed hemorrhaging in the lung and GI tract, bloody chylous ascites, and growth retardation, which resembles the observations in mice with a conditional deletion of *T-synthase* in endothelial and hematopoietic cells (EHC) (19), but future studies using EHC *Cosmc* deletions

will be required to define the role of *Cosmc* in EHC functions. Interestingly, recent studies show that mice with severe loss of T-synthase activity because of N-ethyl-N-nitrosourea-induced mutation develop thrombocytopenia and kidney disease (6). In our *Cosmc* mosaic mice, we observed that some tissues, such as those in the GI tract, had an architecture containing Tn(+) cells that appeared normal, but in other tissues, such as spleen and liver, the architecture of the tissue containing Tn(+) cells was disrupted. This suggests that Tn(+) cells have altered differentiation compared with normal cells. Although Tn(+) cells were present in the glomeruli and proximal and distant tubules in the kidney, we did not observe significant abnormalities there, such as inflammation.

Mosaic mice with a *Cosmc* deletion in a portion of cells in a tissue or an organ resemble several human diseases, such as Tn syndrome, in which somatic, acquired mutations in *Cosmc* are associated with the phenotype of the patients (7, 28). Tn syndrome is characterized by a mixed population of Tn(−) and Tn(+) blood cells of all lineages (29). This mouse model may also be useful in animal studies aimed at modeling the biology of IgA nephropathy, in which a fraction of IgA1 carries the Tn antigen, while the remaining IgA1 carries normal sialyl T antigen in the hinge region (30–33). It has been hypothesized that a small population of plasma cells expressing a mutated *Cosmc* secrete IgA1 with Tn antigen (30). However, mouse IgA, unlike human IgA1, is not O-glycosylated and the creation of a mouse model for IgAN will be complex and require generation of transgenic mice with IgA1-type structures and an O-glycosylated hinge region. Finally, the Tn antigen is one of the most well-recognized tumor antigens, and is expressed in many types of carcinomas. Tn expression is associated with poor prognosis, along with accelerated tumor progression and metastasis (1). Although the advantages for tumor cells carrying Tn antigen are not fully understood, binding of Tn antigen by a C-type lectin, termed MGL, on both dendritic cells and macrophages enhances tolerance to the tumor cells (34–36). Future studies using this animal model can explore whether Tn(+) cells or tissues become more susceptible to mutagenesis in the mosaic animals, and whether Tn(+) cells in vivo have survival and growth privileges.

Materials and Methods

Generation of *Cosmc*⁻/ʸ and *Cosmc*flox/y Mouse ES Cells. We engineered a targeting vector with 3 Lox^P sites in the *Cosmc* allele (Fig. 1A). The selected clone (3A12) was transiently transfected to delete *Cosmc* and the *Neo* gene cassette, generating ES cells with a null *Cosmc* (*Cosmc*⁻/ʸ), or *Neo* gene cassette only to create ES cells with a floxed *Cosmc* (*Cosmc*flox/y).

Generation of *Cosmc*flox/+, *Cosmc* mosaic, *Cosmc*+/−, and *Cosmc*⁻/ʸ Mice, and *Cosmc*+/− and *Cosmc*⁻/ʸ Mouse Embryos. The *Cosmc*⁻/ʸ and *Cosmc*flox/y ES cells were microinjected into C57BL/6J blastocysts, and implanted into pseudopregnant mice. Chimeras among the offspring were bred with C57BL/6J female mice to generate female mice with *Cosmc*flox/+. Genotypes of mice were determined by PCR of DNA from tail biopsies or from portions of embryos or yolk sacs. WT and floxed alleles were identified using PCR with specific primers (Table S3). The strategies for generating the mice or embryos with different genotyping (*Cosmc*flox/+, *Cosmc* mosaic, *Cosmc*+/−, *Cosmc*⁻/ʸ) are shown (Fig. 2A). Genotypes of mice were determined by PCR of DNA from tail snips. (SI Materials and Methods).

1. Byrd JC, Bresalier RS (2004) Mucins and mucin binding proteins in colorectal cancer. *Cancer Metastasis Rev* 23(1–2):77–99.
2. Ju T, Brewer K, D'Souza A, Cummings RD, Canfield WM (2002) Cloning and expression of human core 1 beta1,3-galactosyltransferase. *J Biol Chem* 277(1):178–186.
3. Ju T, Cummings RD (2002) A unique molecular chaperone Cosmc required for activity of the mammalian core 1 beta 3-galactosyltransferase. *Proc Natl Acad Sci USA* 99:16613–16618.
4. Ju T, Aryal RP, Stowell CJ, Cummings RD (2008) Regulation of protein O-glycosylation by the endoplasmic reticulum-localized molecular chaperone Cosmc. *J Cell Biol* 182:531–542.
5. Aryal RP, Ju T, Cummings RD (2010) The endoplasmic reticulum chaperone Cosmc directly promotes in vitro folding of T-synthase. *J Biol Chem* 285:2456–2462.
6. Alexander WS, et al. (2006) Thrombocytopenia and kidney disease in mice with a mutation in the C1galt1 gene. *Proc Natl Acad Sci USA* 103:16442–16447.
7. Ju T, Cummings RD (2005) Protein glycosylation: Chaperone mutation in Tn syndrome. *Nature* 437:1252.
8. Baker DA, et al. (1983) Immunochemical studies on the combining sites of Forssman hapten reactive hemagglutinins from *Dolichos biflorus*, *Helix pomatia*, and *Wistaria floribunda*. *Biochemistry* 22:2741–2750.
9. Novogrodsky A, Lotan R, Ravid A, Sharon N (1975) Peanut agglutinin, a new mitogen that binds to galactosyl sites exposed after neuraminidase treatment. *J Immunol* 115:1243–1248.
10. Ju T, et al. (2008) Human tumor antigens Tn and sialyl Tn arise from mutations in Cosmc. *Cancer Res* 68:1636–1646.
11. Kobata A, Endo T (1992) Immobilized lectin columns: Useful tools for the fractionation and structural analysis of oligosaccharides. *J Chromatogr* 597(1–2):111–122.
12. Cummings RD (1994) Use of lectins in analysis of glycoconjugates. *Methods Enzymol* 230:66–86.
13. Merkle RK, Cummings RD (1987) Lectin affinity chromatography of glycopeptides. *Methods Enzymol* 138:232–259.
14. Shibuya N, et al. (1987) The elderberry (*Sambucus nigra* L.) bark lectin recognizes the Neu5Ac(alpha 2-6)Gal/GalNAc sequence. *J Biol Chem* 262:1596–1601.
15. Amano M, et al. (2010) Threshold in stage-specific embryonic glycotypes uncovered by a full portrait of dynamic N-glycan expression during cell differentiation. *Mol Cell Proteomics* 9:523–537.
16. Tremml G, et al. (1999) Increased sensitivity to complement and a decreased red blood cell life span in mice mosaic for a nonfunctional *Piga* gene. *Blood* 94:2945–2954.
17. Lakso M, et al. (1996) Efficient in vivo manipulation of mouse genomic sequences at the zygote stage. *Proc Natl Acad Sci USA* 93:5860–5865.
18. Xia L, et al. (2004) Defective angiogenesis and fatal embryonic hemorrhage in mice lacking core 1-derived O-glycans. *J Cell Biol* 164:451–459.
19. Fu J, et al. (2008) Endothelial cell O-glycan deficiency causes blood/lymphatic misconnections and consequent fatty liver disease in mice. *J Clin Invest* 118:3725–3737.
20. Ju T, Cummings RD, Canfield WM (2002) Purification, characterization, and subunit structure of rat core 1 Beta1,3-galactosyltransferase. *J Biol Chem* 277(1):169–177.
21. Schietinger A, et al. (2006) A mutant chaperone converts a wild-type protein into a tumor-specific antigen. *Science* 314:304–308.
22. Herscovics A (1999) Importance of glycosidases in mammalian glycoprotein biosynthesis. *Biochim Biophys Acta* 1473(1):96–107.
23. Caffaro CE, Hirschberg CB (2006) Nucleotide sugar transporters of the Golgi apparatus: From basic science to diseases. *Acc Chem Res* 39:805–812.
24. Caffaro CE, Hirschberg CB, Berninsone PM (2006) Independent and simultaneous translocation of two substrates by a nucleotide sugar transporter. *Proc Natl Acad Sci USA* 103:16176–16181.
25. Caramelo JJ, Parodi AJ (2007) How sugars convey information on protein conformation in the endoplasmic reticulum. *Semin Cell Dev Biol* 18:732–742.
26. Jackson CL (2009) Mechanisms of transport through the Golgi complex. *J Cell Sci* 122:443–452.
27. Vembar SS, Brodsky JL (2008) One step at a time: Endoplasmic reticulum-associated degradation. *Nat Rev Mol Cell Biol* 9:944–957.
28. Crew VK, et al. (2008) New mutations in C1GALT1C1 in individuals with Tn positive phenotype. *Br J Haematol* 142:657–667.
29. Berger EG (1999) Tn-syndrome. *Biochim Biophys Acta* 1455:255–268.
30. Julian BA, Novak J (2004) IgA nephropathy: An update. *Curr Opin Nephrol Hypertens* 13(2):171–179.
31. Li GS, Zhang H, Lv JC, Shen Y, Wang HY (2007) Variants of *C1GALT1* gene are associated with the genetic susceptibility to IgA nephropathy. *Kidney Int* 71:448–453.
32. Hiki Y (2009) O-linked oligosaccharides of the IgA1 hinge region: roles of its aberrant structure in the occurrence and/or progression of IgA nephropathy. *Clin Exp Nephrol* 13:415–423.
33. Zhu L, et al. (2009) Interaction between variants of two glycosyltransferase genes in IgA nephropathy. *Kidney Int* 76:190–198.
34. Napoletano C, et al. (2007) Tumor-associated Tn-MUC1 glycoform is internalized through the macrophage galactose-type C-type lectin and delivered to the HLA class I and II compartments in dendritic cells. *Cancer Res* 67:8358–8367.
35. Saeland E, et al. (2007) The C-type lectin MGL expressed by dendritic cells detects glycan changes on MUC1 in colon carcinoma. *Cancer Immunol Immunother* 56:1225–1236.
36. Singh SK, et al. (2009) Characterization of murine MGL1 and MGL2 C-type lectins: Distinct glycan specificities and tumor binding properties. *Mol Immunol* 46:1240–1249.

DEVELOPMENTAL BIOLOGY